Journal of Computational Applied Mechanics 2024, 55 (-): PP-PP

DOI:10.22059/JCAMECH.2024.369060.914

RESEARCH PAPER

Fuzzy logic-based variable impedance control for a bilateral teleoperation system under time delay

Maryam Raeisi Sarkhooni [a], Behnam Yazdankhoo [a], Mohammad Reza Hairi Yazdi [a,*], Farshid Najafi [b]

[a] *School of Mechanical Engineering, College of Engineering, University of Tehran, Tehran, Iran.*
[b] *School of Mechatronic Systems Engineering, Faculty of Applied Sciences, Simon Fraser University, British Columbia, Canada.*

Abstract

In a delayed master-slave teleoperation system, if the slave robot interacts with a delicate and sensitive environment, it is essential to control the slave-environment interactions. Variable impedance control has been proposed as a useful method for this aim in the literature. However, changing the impedance parameters based on the system requirements imposes a complex process in the controller design. To address this issue, we propose a variable impedance control strategy for the slave side, where the impedance variables are changed using fuzzy logic. This is carried out based on the environment destruction threshold—defined based on the contact force and the velocity of the slave robot—and system stability range. The proposed method is simulated in MATLAB's Simulink considering telesurgery conditions and soft tissue environment under an unknown and varying time delay. Simulation results show that the proposed method maintains the velocity of the slave robot and the environment force in the desired interval and performs better in keeping the environment safe compared to the constant-coefficient impedance control.

Keywords: teleoperation; time delay; variable impedance control; absolute stability; fuzzy logic

1. Introduction

Teleoperation systems solve the distance limitation problems and remove the risk of direct contact with dangerous environments. Medical, space, nuclear, and underwater industries are some of the applications of teleoperation systems [1]. A teleoperation system consists of five subsystems: the operator, the master robot and its controller, the communication channel, the slave robot and its controller, and the environment. The communication channel may have time delays, and make the system unstable. Albeit, the delays in teleoperation systems could stem from three different sources: Signal transmission, computation and mechanical delay [2]. We, however, focus on the transmission latency in this work.

Because of the inevitable trade-off between stability and transparency, having the desired stability and

* Corresponding author. Tel.: (+98-21) 61119916; fax: (+98-21) 88013029.
E-mail address: myazdi@ut.ac.ir

transparency during performance has always been one of the goals in designing a controller for bilateral teleoperation systems. Making the controller robust to uncertainties, reducing the oscillations in moves, and enhancing the system performance in the presence of time delays in communication channels are other goals that have been considered in designing the controller. Moreover, modeling different parts of the system, for instance human-robot interaction, has recently been investigated in the literature [3].

One of the easiest control methods, i.e., PID controller, has been implemented in bilateral teleoperation systems [4]. The advantages of implementing a PID controller are the simplicity and straightforward design, but sudden moves or variable time delays can make the system unstable.

To make the controller robust to model uncertainties and time delay, sliding-mode control [5] or optimal disturbance rejection-based robust control methods [6] can be used. To cope with time delay and improve stability and transparency, predictive control approaches can be utilized, either on the master side for the prediction of the movement of the human operator [7, 8], or on the slave side for predicting the interaction force between the slave robot and the remote environment system [9]. The human intent prediction indeed covers a wide spectrum of studies and is still an ongoing research topic [10].

Model-free schemes such as neural-network-based control can also be implemented to cope with time delay and system uncertainties [11]. Using the learning capabilities of artificial neural networks, uncertainties can be estimated and used to improve performance. Adaptive control is another approach that can be employed solely [12] or in combination with other control methods to control delayed teleoperation systems [13]. Controlling the convergence time of the tracking error, employing a neural network-based adaptive terminal sliding mode control, is another solution provided for dealing with the negative effects of time delays and improving the performance of the system [14].

The aforementioned control approaches aim at synchronizing the positions of the master and slave robots. In the case of a sensitive environment, however, it is also important to control the contact force while the slave robot is interacting with it because it may cause damage to the environment. To control the contact force, impedance control, which defines a dynamic relation between the contact force and the velocity of the robot, is proposed. The main and well-known usage of impedance control in teleoperators might be providing the operator with a proper haptic feel on the master side.

In recent years, however, many researches have proposed incorporating impedance control on the slave side to keep the remote contact force in control. Adaptive impedance control utilizing Learning from Demonstration (LfD) [15], robust L_1-based impedance control [16], and model-reference adaptive impedance control [17] are examples of such works. Impedance control has also been used in combination with other control strategies, such as sliding mode [18] and neural fuzzy inference system (ANFIS) [19], to improve the performance of the whole system.

Many of the proposed impedance-based architectures in the literature assume the target impedance behavior remains constant throughout the operation. This design might be sufficient for the conditions where the environment is known a priori; however, interaction with variable, unstructured, or fragile environments requires extra caution from the controller design point of view, since the operator may unintentionally damage the remote environment. Variable impedance control has been proposed as a promising approach to tackle this issue in robotic systems [20, 21], where the desired impedance parameters are designed to be changed in response to different contact conditions. In the context of teleoperation systems, a variable impedance control approach has been applied to the master side [1, 22]; however, modifying the target impedance based on the contact conditions on the slave side is an issue which is overlooked.

In the literature, fuzzy logic has been previously implemented in robotic systems control [23] and in telerobotic systems to deal with time delay [24]. Providing a human-like control interface, fuzzy logic method can help a variable impedance controller be designed in which the parameters are smoothly changed in a manner similar to how an operator would perform if he/she were supposed to directly interact with the environment. This idea has recently been carried out successfully for the master side in a teleoperation system to modify the impedance/admittance control structure [22]. However, implementing a variable impedance control scheme on the slave side of a telerobotic system, which could result in a safe interaction with the environment, is not considered in the literature yet. Indeed, variable impedance control, in combination with fuzzy logic on the slave side, seems to properly address the issues regarding safe remote interaction in the presence of time delay and gives us the ability to control the remote robot to prevent damage to the environment.

Therefore, the main contribution of this paper is introducing a variable impedance control structure for the slave robot in a teleoperation system with unknown, variable time delay using the fuzzy logic method. The goal is to keep the slave robot's velocity and contact force below predefined values based on the environment destruction threshold to prevent any potential damage to the environment. Changing the coefficients of the desired impedance equation based on fuzzy logic also incorporates the stability condition of the system (using absolute stability criterion), where

the process of tuning the parameters based on stability condition is also explained.

This paper is structured as follows. Section 2 contains the system structure and model dynamics. In Section 3, the stability method is discussed. Section 4 describes the proposed method, concluding the stability criterion of the teleoperation system under a time delay. Simulation results with a 1-DOF teleoperation system are shown in Section 5, followed by conclusions in Section 6.

2. System structure and model dynamics

The teleoperation system consists of two robots, one on the master side and the other on the slave side. Two sides send signals through communication channels with variable time delay. The operator applies force to the master robot and manipulates the master robot, the delayed signals are received at the slave side, and the slave robot moves to track the master position. In **Error! Reference source not found.** the teleoperation system structure is illustrated. x_m is the master position, f_h is the human force applied to the master robot and f_e is the environment force sensed by the slave robot. The delayed signals are ${x_m}^d = x_m(t - T_1(t))$, ${\dot{x}_m}^d = \dot{x}_m(t - T_1(t))$, ${f_h}^d = f_h(t - T_1(t))$ and ${f_e}^d = f_e(t - T_2(t))$.

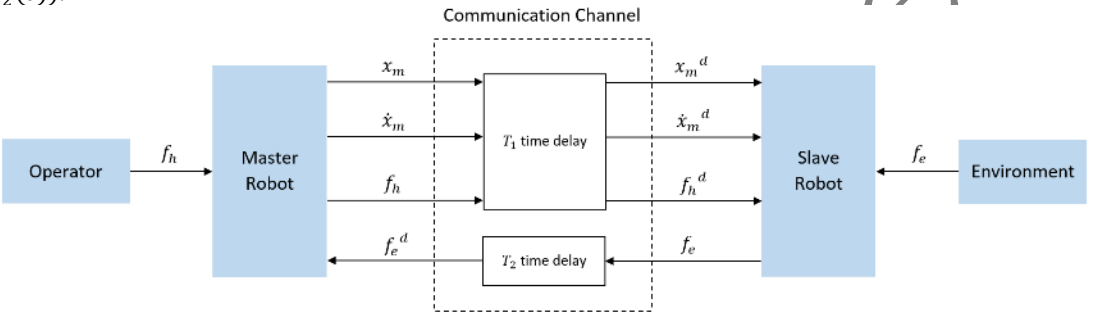

Fig 1: general teleoperation system structure

2.1. Master and slave robots' dynamics

The master and slave robots are modelled as a 1-DOF mass-damper system, modelled in equation (1) and equation (2).

$$m_m\ddot{x}_m(t) + b_m\dot{x}_m(t) = u_m(t) + f_h(t) \quad (1)$$

$$m_s\ddot{x}_s(t) + b_s\dot{x}_s(t) = u_s(t) - f_e(t) \quad (2)$$

where x_s is the slave position, m_m and m_s are the master and slave inertia, b_m and b_s are master and slave damping, u_m and u_s are the controller outputs for master and slave. The transmitted signals can be scaled by multiplying the signals to position and force scaling factors k_p and k_f respectively.

2.2. Master robot impedance control

The impedance controller for the master robot defines a desired dynamic behavior between a human operator and the master robot. The impedance equation for the master robot is defined in equation (3):

$$\bar{m}_m\ddot{x}_m(t) + \bar{b}_m\dot{x}_m(t) + \bar{k}_m x_m(t) = f_h(t) - k_f {f_e}^d(t) \quad (3)$$

where $\bar{m}_m$, $\bar{b}_m$ and $\bar{k}_m$ are desired mass, damping and stiffness coefficients, respectively. By eliminating $\ddot{x}_m$ in equation (1) and equation (3), master controller output u_m can be obtained.

$$u_m(t) = \left(b_m - \frac{m_m}{\bar{m}_m}\bar{b}_m\right)\dot{x}_m(t) + \left(\frac{m_m}{\bar{m}_m} - 1\right)f_h(t) - \frac{m_m}{\bar{m}_m}\left(k_f {f_e}^d(t) + \bar{k}_m x_m(t)\right) \quad (4)$$

2.3. Slave robot variable impedance control

Impedance controller for the slave robot is supposed to define a desired behavior between slave tracking error and the environment force. The impedance equation for the slave robot is defined in equation (5):

$$\bar{m}_s \ddot{\tilde{x}}_s(t) + \bar{b}_s \dot{\tilde{x}}_s(t) + \bar{k}_s \tilde{x}_s(t) = -f_e(t) \tag{5}$$

where $\bar{m}_s$, $\bar{b}_s$ and $\bar{k}_s$ are desired mass, damping and stiffness coefficients, respectively. And $\tilde{x}_s(t) = x_s(t) - k_p {x_m}^d(t)$. Slave controller output can be obtained from equation (2) and equation (5):

$$u_s(t) = \left(b_s - \frac{m_s}{\bar{m}_s}\bar{b}_s\right)\dot{x}_s(t) + \left(1 - \frac{m_s}{\bar{m}_s}\right) f_e(t) - \frac{m_s}{\bar{m}_m} k_p \left(k_f {f_e}^{dd}(t) - {f_h}^d(t)\right) - \frac{m_s}{\bar{m}_s}\bar{k}_s x_s(t) + \left(\frac{\bar{b}_s}{\bar{m}_s} - \frac{\bar{b}_m}{\bar{m}_m}\right) m_s k_p \dot{x}_m{}^d(t) + \left(\frac{\bar{k}_s}{\bar{m}_s} - \frac{\bar{k}_m}{\bar{m}_m}\right) m_s k_p x_m{}^d(t) \tag{6}$$

where ${f_e}^{dd}(t) = {f_e}^d(t - T_1(t)) = f_e(t - T_1(t) - T_2(t))$. An overview of the teleoperation system is illustrated in **Error! Reference source not found.**.

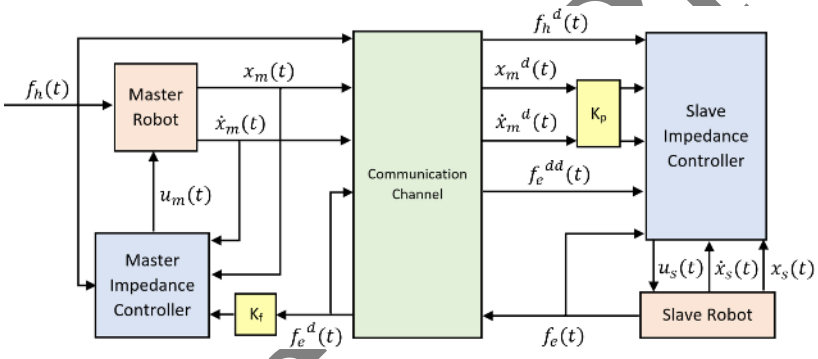

Fig 2: Overview of the teleoperation system

3. Stability of the teleoperation system

The absolute stability criterion is used to analyze the delayed teleoperation system. To use this criterion, first, the teleoperation system has to be defined as a two-port network with two inputs and two outputs due to interacting with the human operator and the environment. In **Error! Reference source not found.**, the mentioned two-port network is illustrated.

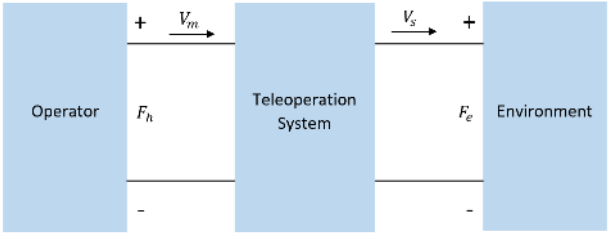

Fig 3: A delayed teleoperation system defined as a two-port network

The relation between inputs and outputs can be defined by a hybrid matrix:

$$\begin{bmatrix} F_h \\ -V_s \end{bmatrix} = \begin{bmatrix} h_{11} & h_{12} \\ h_{21} & h_{22} \end{bmatrix} \begin{bmatrix} V_m \\ F_e \end{bmatrix} \tag{7}$$

where F_h, V_s, V_m and F_e are the Laplace transforms of f_h, $\dot{x}_s$, $\dot{x}_m$ and f_e. The hybrid matrix elements can be obtained by the dynamic models and desired impedance equations defined for master and slave robot, which are $h_{11} = \bar{m}_m s + \bar{b}_m + \frac{\bar{k}_m}{s}$, $h_{12} = k_f e^{-T_2 s}$, $h_{21} = -k_p e^{-T_1 s}$ and $h_{22} = \frac{s}{\bar{m}_s s^2 + \bar{b}_s s + \bar{k}_s}$.

The absolute stability is defined as:

A linear two-port is said to be absolutely stable if no set of passive terminating one-port impedance exists for which the system is unstable. If the network is not absolutely stable, it is potentially unstable.

A necessary and sufficient condition for the absolute stability of a two-port network is that one-port networks, resulting from any passive output and input termination, are themselves passive. Llewellyn's stability criteria provide the necessary and sufficient conditions for the absolute stability:

a) h_{11} and h_{22} have no poles in the right half plane.

b) Any poles of h_{11} and h_{22} on the imaginary axis are simple with real and positive residues.

c) For all real values of ω: $Re[h_{11}] \geq 0$, $Re[h_{22}] \geq 0$ and $f(\omega) = 2Re[h_{11}]Re[h_{22}] - Re[h_{12}h_{21}] - |h_{12}h_{21}| \geq 0$ should be satisfied.

The (a) and (b) criteria are satisfied as the desired impedance coefficients are always positive. The terms for (c) criteria can be written as:

$$Re[h_{11}] = \bar{b}_m \tag{8}$$

$$Re[h_{22}] = \frac{\bar{b}_s \omega^2}{(\bar{k}_s - \bar{m}_s \omega^2)^2 + (\bar{b}_s \omega)^2} \tag{9}$$

$$f(\omega) = [cos([T_1(t) + T_2(t)]\omega) - 1]k_p k_f + \frac{2\bar{b}_m \bar{b}_s \omega^2}{(\bar{k}_s - \bar{m}_s \omega^2)^2 + (\bar{b}_s \omega)^2} \geq 0 \tag{10}$$

(8) and (9) are satisfied as the desired impedance coefficients are always positive. The third term, equation (10), needs to be satisfied in the interval the coefficient change happens. It is noteworthy that among all the criteria mentioned for absolute stability, the time delays merely appear in equation (10), which is further analyzed in the next section.

4. Changing the coefficients

The transfer function of the slave robot desired impedance equation can be written as:

$$\frac{\bar{x}_s(s)}{-F_e(s)} = \frac{1}{\bar{m}_s s^2 + \bar{b}_s s + \bar{k}_s} = \frac{gain \times {\omega_n}^2}{s^2 + 2\zeta\omega_n s + {\omega_n}^2} \tag{11}$$

and equation (12) can be obtained:

$$\bar{m}_s = \frac{1}{gain\ {\omega_n}^2}, \bar{b}_s = \frac{2\zeta}{gain\ \omega_n}, \bar{k}_s = \frac{1}{gain} \tag{12}$$

where ζ, ω_n and $gain$ are the damping ratio, natural frequency and steady-state gain of the transfer function, respectively. By changing these parameters instead of $\bar{m}_s$, $\bar{b}_s$ and $\bar{k}_s$ we can have the advantage of choosing $\zeta = 1$ to determine the fastest non-oscillating response for the slave robot. Also, because the role ω_n and $gain$ play in determining the behavior is known, we can have the notion that increasing $gain$ will increase the error position, and increasing ω_n will increase the robot reaction velocity.

Note that setting $\zeta = 1$ is an arbitrary choice in order to lead the procedure of modulating the coefficients to a more convenient one for the other two parameters, namely ω_n and $gain$. In other words, not only will it yield to a critically damped response, but also it will reduce the modulating parameters to two. While selecting other values for ζ is also possible, any other choice other than 1 will make the response either too slow or oscillating, which should be further compensated by ω_n. Furthermore, considering ζ as a variable will result in a more complicated design process.

4.1. Admissible interval for target impedance parameters

To determine the changing interval for ω_n and $gain$, equation (10) needs to be considered. In equation (10) the interval of ω also matters, and thus, first we need to determine the frequency interval. To do that, because the variable time delays exist as the argument of the cosine term, equation (10) is simplified:

$$k_p k_f \leq \frac{\bar{b}_m \bar{b}_s \omega^2}{(\bar{k}_s - \bar{m}_s \omega^2)^2 + (\bar{b}_s \omega)^2} \tag{13}$$

Equation (13) is a quadratic equation in terms of ω. The interval of ω in which equation (13) is satisfied can be obtained as:

$$\omega_{1,2}{}^2 = \frac{\bar{k}_s}{\bar{m}_s} + \frac{\bar{b}_m \bar{b}_s}{k_p k_f 2\bar{m}_s{}^2} - \frac{\bar{b}_s{}^2}{2\bar{m}_s{}^2} \pm \sqrt{\frac{\bar{b}_s{}^4}{4\bar{m}_s{}^4} + \frac{\bar{b}_m{}^2 \bar{b}_s{}^2}{k_p{}^2 k_f{}^2 4\bar{m}_s{}^4} - \frac{\bar{b}_m \bar{b}_s{}^3}{k_p k_f 2\bar{m}_s{}^4} - \frac{\bar{b}_s{}^2 \bar{k}_s}{\bar{m}_s{}^3} + \frac{\bar{b}_m \bar{b}_s \bar{k}_s}{k_p k_f \bar{m}_s{}^3}} \tag{14}$$

To have a frequency interval equation (15) needs to be satisfied.

$$0 < \bar{b}_s < \frac{\bar{b}_m}{k_p k_f} \tag{15}$$

Equation (14) written in ζ, ω_n and $gain$ is obtained as:

$$\omega_{1,2}{}^2 = \omega_n{}^2 \left[1 + \left(\frac{\bar{b}_m}{k_p k_f}\zeta\right)(gain\omega_n) - 2\zeta^2\right] \pm$$
$$\omega_n{}^2 \sqrt{4\zeta^4 + (\frac{\bar{b}_m}{k_p k_f}\zeta)^2 (gain\omega_n)^2 - (\frac{4\bar{b}_m}{k_p k_f}\zeta^3)(gain\omega_n) - 4\zeta^2 + (\frac{2\bar{b}_m}{k_p k_f}\zeta)(gain\omega_n)} \tag{16}$$

As can be seen in equation (16) changing term ($gain\omega_n$) can change the interval of frequency $[\omega_1, \omega_2]$. In order to determine a single frequency interval for system, ω_{1max} and $\omega_{2\,min}$ will be obtained using a constraints optimization solution. But first the changing interval of ω_n and $gain$ have to be determined.

Equation (15) written in terms of ζ, ω_n and $gain$ is obtained as $0 < \frac{2\zeta}{gain\ \omega_n} < \frac{\bar{b}_m}{k_p k_f}$ and by setting $\zeta = 1$, one has

$$gain\ \omega_n > \frac{2k_p k_f}{\bar{b}_m} \tag{17}$$

$gain_{min}$ and $\omega_{n\,min}$ allowed by stability criteria is defined by equation (17). But determining $gain_{max}$ and $\omega_{n\,max}$ does not need any consideration of stability criteria.

After determining an interval for ω_n and $gain$ to change, frequency interval will be obtained by equation (16). If the frequency interval is not desired, it should be considered that equation (16) is obtained by simplifying equation (10), so it results in a tighter frequency interval. Equation (10) written in terms of ζ, ω_n and $gain$ is obtained as:

$$f(\omega, gain, \omega_n, T_1, T_2) = [\cos([T_1 + T_2]\omega) - 1]k_p k_f + \frac{4\bar{b}_m \zeta\left(\frac{\omega^2}{\omega_n}\right) gain}{\left(1 - \left(\frac{\omega}{\omega_n}\right)^2\right)^2 + 4\zeta^2\left(\frac{\omega}{\omega_n}\right)^2} \geq 0 \tag{18}$$

If equation (18) is satisfied in the difference between the desired and calculated frequency intervals, the desired frequency interval can be considered as the system frequency interval, but if equation (18) is not satisfied, the intervals chosen for ω_n and $gain$ have to change. To determine how changing the interval will affect the frequency, $\frac{\partial f(\omega, gain, \omega_n, T_1, T_2)}{\partial gain}$ and $\frac{\partial f(\omega, gain, \omega_n, T_1, T_2)}{\partial \omega_n}$ is calculated.

$$\frac{\partial f(\omega, gain, \omega_n, T_1, T_2)}{\partial gain} = \frac{4\bar{b}_m \zeta\left(\frac{\omega^2}{\omega_n}\right)}{\left(1 - \left(\frac{\omega}{\omega_n}\right)^2\right)^2 + 4\zeta^2\left(\frac{\omega}{\omega_n}\right)^2} \tag{19}$$

$$\frac{\partial f(\omega,gain,\omega_n,T_1,T_2)}{\partial \omega_n}=\frac{\left(-4b_m\zeta\frac{\omega^2}{{\omega_n}^2}gain\right)\left(1-3\frac{\omega^4}{{\omega_n}^4}+2\frac{\omega^2}{{\omega_n}^2}-4\zeta^2\frac{\omega^2}{{\omega_n}^2}\right)}{\left(\left(1-\left(\frac{\omega}{\omega_n}\right)^2\right)^2+4\zeta^2\left(\frac{\omega}{\omega_n}\right)^2\right)^2} \tag{20}$$

To investigate the sign of the equation (20), $\zeta = 1$ is set:

$$\frac{\partial f(\omega,gain,\omega_n,T_1,T_2)}{\partial \omega_n}=\frac{\left(-4b_m\frac{\omega^2}{{\omega_n}^2}gain\right)\left(-3\frac{\omega^4}{{\omega_n}^4}-2\frac{\omega^2}{{\omega_n}^2}+1\right)}{\left(\left(1+\left(\frac{\omega}{\omega_n}\right)^2\right)^2\right)^2} \tag{21}$$

Equation (19) is always positive, so to increase $f(\omega, gain, \omega_n, T_1, T_2)$, $gain_{min}$ should be increased. The sign of the equation (21) depends on the magnitude of $\frac{\omega^2}{{\omega_n}^2}$, when $\frac{\omega^2}{{\omega_n}^2} > \frac{1}{3}$ equation (21) is positive and when $\frac{\omega^2}{{\omega_n}^2} < \frac{1}{3}$ equation (21) is negative. Hence, if $\omega_{n_{max}} < \sqrt{3}\omega_1$ equation (21) is positive and to increase $f(\omega, gain, \omega_n, T_1, T_2)$, $\omega_{n_{min}}$ should be increased. If $\omega_{n_{min}} > \sqrt{3}\omega_2$ equation (21) is negative and to increase $f(\omega, gain, \omega_n, T_1, T_2)$, $\omega_{n_{max}}$ should be decreased. A summary of how to change ω_n and $gain$ intervals is written in Table 1.

Table 1: Guide to change ω_n and $gain$ intervals to satisfy stability criterion

Derivative function	sign	solution
$\frac{\partial f(\omega, gain, \omega_n, T_1, T_2)}{\partial gain}$	Always positive	Increasing $gain_{min}$
$\frac{\partial f(\omega, gain, \omega_n, T_1, T_2)}{\partial \omega_n}$	$\frac{\omega^2}{{\omega_n}^2} > \frac{1}{3} \rightarrow$ positive	Increasing $\omega_{n_{min}}$
	$\frac{\omega^2}{{\omega_n}^2} < \frac{1}{3} \rightarrow$ negative	Decreasing $\omega_{n_{max}}$

A flowchart to find a desired interval for ω_n, $gain$ and ω is shown in **Error! Reference source not found.**.

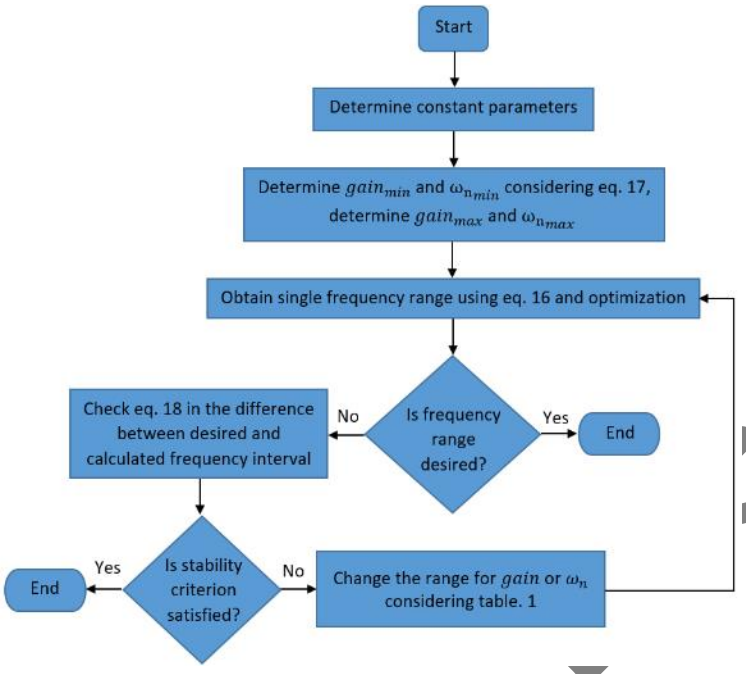

Fig 4: Flowchart to find a desired interval for ω_n, $gain$ and ω

4.2. Changing target impedance parameters

Fuzzy logic is used to change the variables. As the goal is to keep the environment force and slave robot's velocity at the defined limit, the environment force, and slave robot's velocity are the input, and ω_n and $gain$ are the output variables. Generally, when environment force and the robot's velocity are in the normal interval, it is expected to get minimum ω_n and $gain$, but when they get close to the limit, it is expected to get greater ω_n and $gain$ so that the robot moves slower. **Error! Reference source not found.** illustrates an overview of the fuzzy logic function.

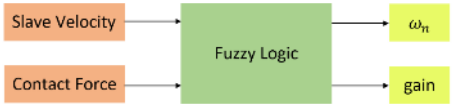

Fig 5: Overview of the fuzzy logic function

Mamdani algorithm is chosen for fuzzy inference system. Outputs crisp values are defuzzified by the centroid method. The membership function of each fuzzy set is the Gbell type function to have the smoothest transition between each set [25], because even small oscillations in the gain output results in significant oscillations in the slave controller output. Gbell functions are defined in equation (22).

$$f(x;a,b,c) = \frac{1}{1+\left|\frac{x-c}{a}\right|^{2b}} \tag{22}$$

If input intervals for velocity and force are defined as *normal:* $[0,\theta_{normal}]$, *cautious:* $[\theta_{normal},\theta_{cautious}]$, *limit:* $[\theta_{cautious},\theta_{limit}]$ and *safety limit:* $[\theta_{limit},n\theta_{limit}]$, where θ corresponds to velocity and force and n is a real number greater than 1, membership function parameters are chosen as shown in **Error! Reference source not found.**. For the initial and last membership functions, 'a' is equal to the interval length and 'c' is equal to the minimum of the interval of the first membership function and the maximum of the interval of the last membership function, respectively. For the other ones, 'a' is equal to the half of the interval length and 'c' is equal to the average of the interval. The peak length and the slope of the function depend on the amount of 'b', which is selected by trial-and-error process.

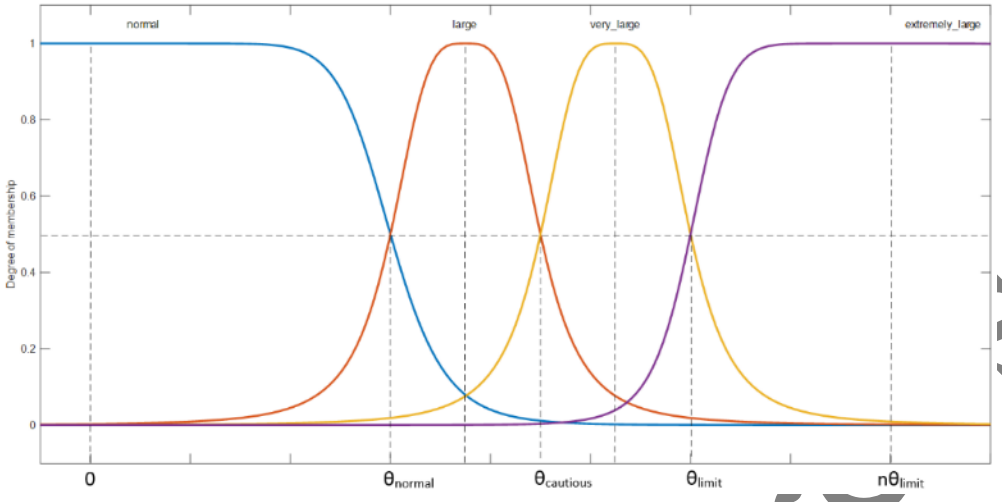

Fig 6: Determining inputs membership functions

Error! Reference source not found. and **Error! Reference source not found.** illustrate how to define the output membership functions. They are set symmetrically at first and modified or moved a bit to get the desired results by trial and error.

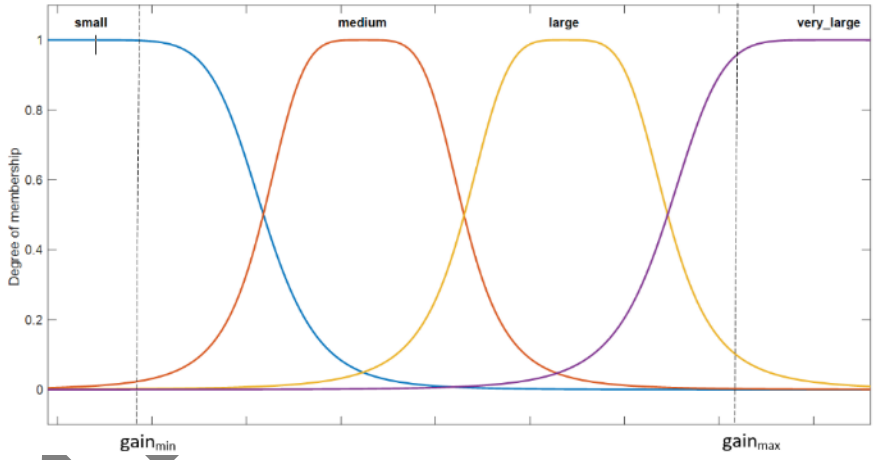

Fig 7: Determining *gain* membership functions

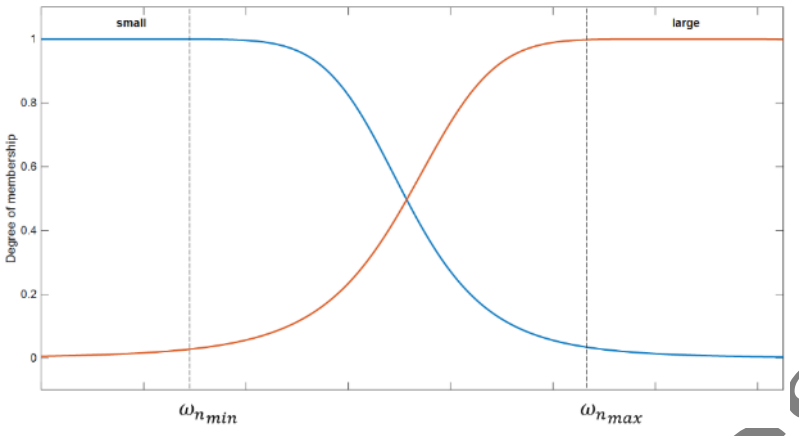

Fig 8: Determining ω_n membership functions

The fuzzy logic rules are defined to have the desired behavior as:

$$\theta_i \rightarrow \text{cautious interval}$$

$$\begin{cases} v < v_{limit} - \theta_v \rightarrow \text{normal error} \\ v_{limit} - \theta_v < v < v_{limit} \rightarrow \text{more error (be cautious)} \\ v > v_{limit} \rightarrow \text{more error to keep the velocity at } v_{limit} \end{cases}$$

$$\begin{cases} f_e < f_{e\,limit} - \theta_{f_e} \rightarrow \text{normal error} \\ f_{e\,limit} - \theta_{f_e} < f_e < f_{e\,limit} \rightarrow \text{more error (be cautious)} \\ f_e > f_{e\,limit} \rightarrow \text{more error to keep the force at } f_{e\,limit} \end{cases}$$

For the inputs, four membership functions are chosen:

Normal: contains the expected interval
Large: contains the cautious interval
Very large: contains the limit interval
Extremely large: contains the safety factor limit interval

For the outputs, *gain* has four membership functions as:

Small: corresponding to the normal input
Medium: corresponding to the large input
Large: corresponding to the very large input
Very large: corresponding to the extremely large input

And ω_n has two membership functions as:

Small: corresponding to the normal input
Large: corresponding to the large, very large and extremely large input

And the rules are defined as:

1. (f_e extremely large) or (v_s extremely large) → (ω_n large) and (*gain* very large)
2. (v_s normal) and (f_e not extremely large) → (ω_n small) and (*gain* small)
3. (v_s large) and (f_e not extremely large) → (ω_n large) and (*gain* medium)
4. (v_s very large) and (f_e not extremely large) → (ω_n large) and (*gain* large)
5. (f_e normal) and (v_s not extremely large) → (ω_n small) and (*gain* small)

6. (f_e large) and (v_s not extremely large) → (ω_n large) and (*gain* medium)
7. (f_e very large) and (v_s not extremely large) → (ω_n large) and (*gain* large)

5. Simulation results

The proposed control strategy is simulated in MATLAB's Simulink environment. with the constant parameters gathered in Table 2. It should be noted that the dynamical properties of the master and slave robots are considered to be identical to the Novint Falcon haptic device, which is determined by the system identification process explained in [26].

Table 2: Constant parameters in simulation [26]

parameter	value	unit
m_m	$\frac{1}{1.289}$	kg
b_m	$\frac{37.1}{1.289}$	Ns/m
k_m	0	N/m
m_s	$\frac{1}{1.289}$	kg
b_s	$\frac{37.1}{1.289}$	Ns/m
k_s	0	N/m
$\bar{m}_m$	0.8	kg
$\bar{b}_m$	40	Ns/m
$\bar{k}_m$	0	N/m
k_p	1	-
k_f	1	-
$T_1 + T_2$	≤ 0.6	s

The environment behavior is modelled by equation (23) to simulate the environment force of cutting a liver [27].

$$f_e = \begin{cases} 0 & x < 0 \\ \frac{1}{11.2}\left(e^{\frac{x}{5.5}} - 1\right) & 0 \le x \le 21mm \\ 0.99\,x^2 - 44.245\,x + 496.53 & 21mm \le x \le 23.5mm \\ \frac{1}{20}\left(e^{\frac{x}{20}} + 67\right) & x > 23.5mm \end{cases} \quad (23)$$

Chosen Intervals for ω_n and $gain$ are gathered in Table 3.

Table 3: chosen intervals for ω_n and $gain$

variable	interval
ω_n	$[7, 15] rad/s$
$gain$	$[0.017, 0.05] m/N$

And the system frequency calculated using equation (16) is $[3.50, 19.02] rad/s$.

Considering that a minimum frequency of 3.50 rad/s for telesurgery conditions is higher than the actual value, the desired frequency interval is the one that can contain low frequencies, e.g. [0,3.50] rad/s. The stability condition is checked by equation (18) using a constraint optimization solution in the intervals gathered in Table 4.

Table 4: variables' constraints in optimization

variable	interval
ω_n	$[7, 15] rad/s$
$gain$	$[0.017 , 0.05] m/N$
ω	$[0, 3.50] rad/s$
$T_1 + T_2$	$[0, 0.6] s$

The stability condition is satisfied, so the whole interval of [0, 19.02] rad/s can be considered as system frequency. Chosen intervals for inputs membership functions are gathered in Table 5 and Table 6.

Table 5: Slave robot's velocity intervals

Interval name	Interval value (m/s)
Normal	$[0, 0.025]$
Large	$[0.025, 0.030]$
Very large	$[0.030, 0.035]$
Extremely large	$[0.035, 0.045]$

Table 6: Environment force intervals

Interval name	Interval value (N)
Normal	$[0, 3]$
Large	$[3, 4.5]$
Very large	$[4.5, 5.2]$
Extremely large	$[5.2, 6.5]$

Therefore, their corresponding membership function parameters will be as gathered in Table 7 and Table 8.

Table 7: Slave robot's velocity membership function parameters

Membership function name	Membership function parameter [a b c]
Normal	[0.025 17.2 0]
Large	[0.0025 1 0.0275]
Very large	[0.0025 1 0.0325]
Extremely large	[0.01 6 0.045]

Table 8: Environment force membership function parameters

Membership function name	Membership function parameter [a b c]
Normal	[3 8.7 0]
Large	[0.75 1.8 3.75]
Very large	[0.35 1.8 4.85]
Extremely large	[1.3 5 6.5]

The corresponding membership functions for inputs are illustrated in **Error! Reference source not found.** and **Error! Reference source not found.**.

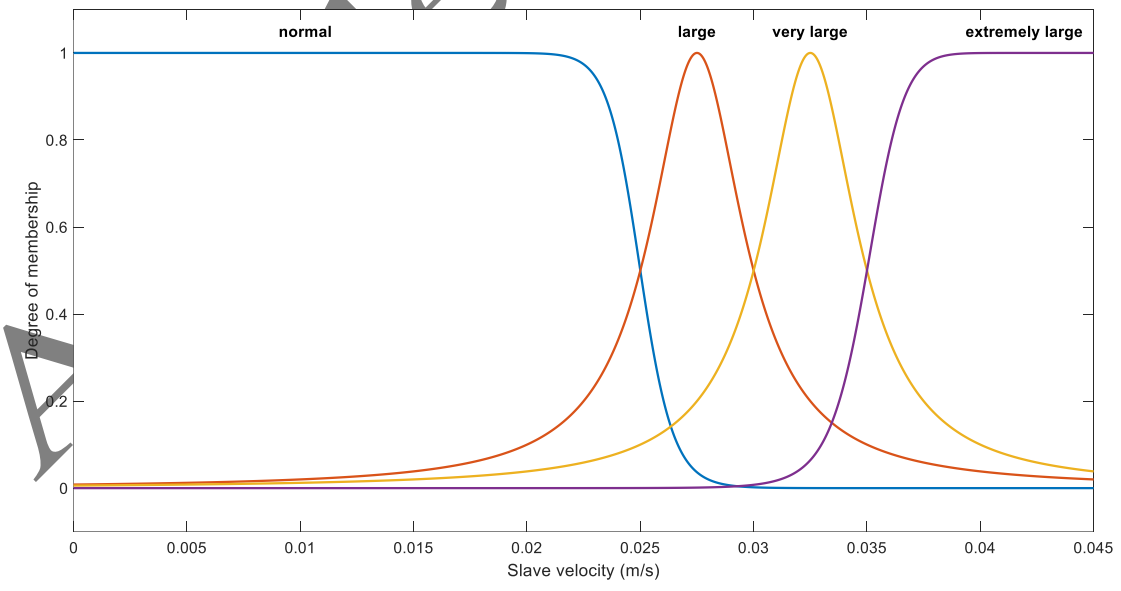

Fig 9: Slave velocity membership functions

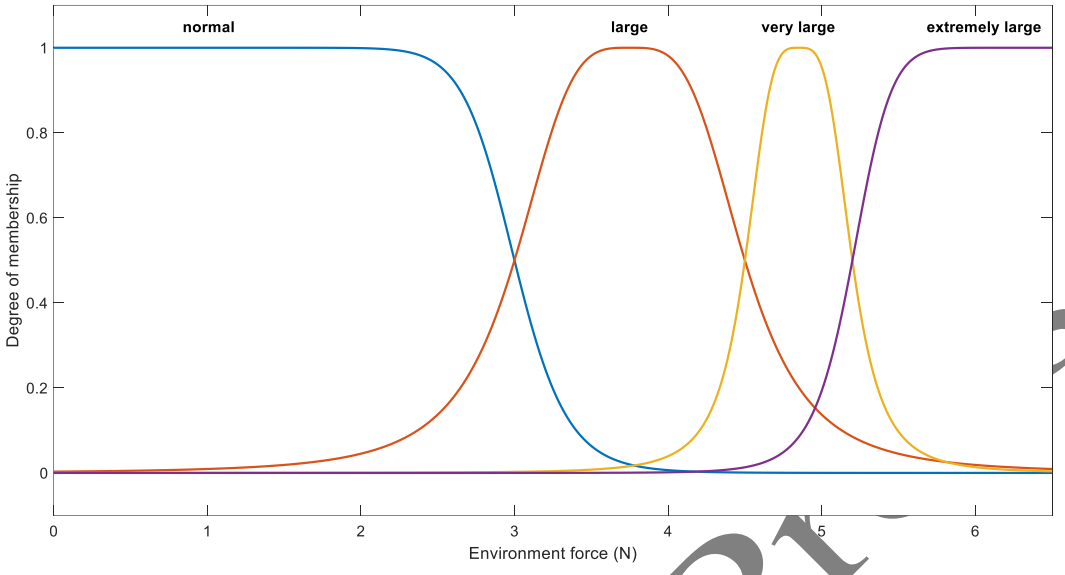

Fig 10: Environment force membership functions

Chosen membership function parameters for the outputs are gathered in Table 9 and Table 10.

Table 9: ω_n membership function parameters

Membership function name	Membership function parameter [a b c]
Small	[4.824 2.75 5.69]
Large	[5.47 2.11 17.45]

Table 10: *gain* membership function parameters

Membership function name	Membership function parameter [a b c]
Small	[0.0045 2.8 0.015]
Medium	[0.004 2 0.025]
Large	[0.0045 1.6 0.036]
Very large	[0.02 6.32 0.062]

The corresponding membership functions for outputs are illustrated in **Error! Reference source not found.** and **Error! Reference source not found.**.

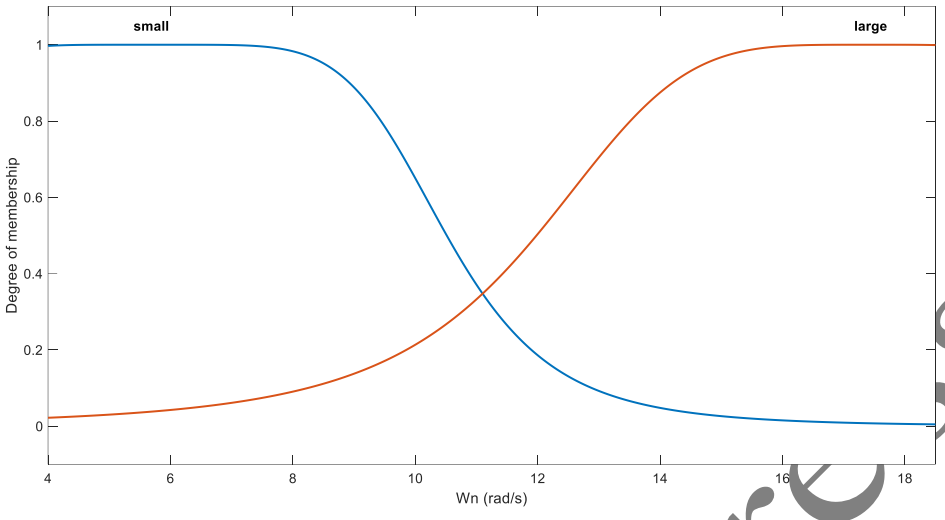

Fig 11: ω_n membership functions

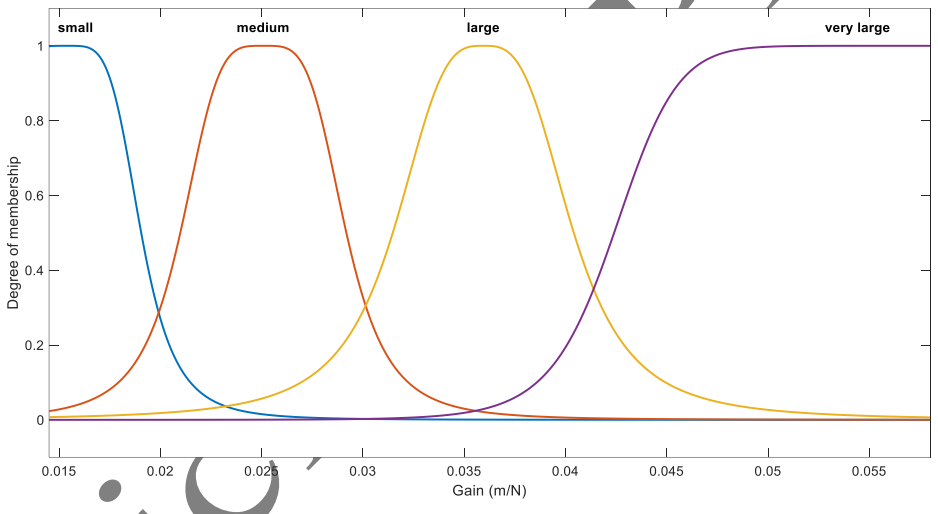

Fig 12: $gain$ membership functions

The results are gathered by inserting operator's force to the master robot as in equation (24).

$$f_h(t) = \begin{cases} 2.75t & 0 < t \leq 2 \\ 5.5 & t > 2 \end{cases} \tag{24}$$

To compare the performance of the proposed variable impedance control method with the constant impedance control method, the result for the same condition but with constant ω_n and $gain$ are shown. Figures 13 to 18 illustrate the main results in this section.

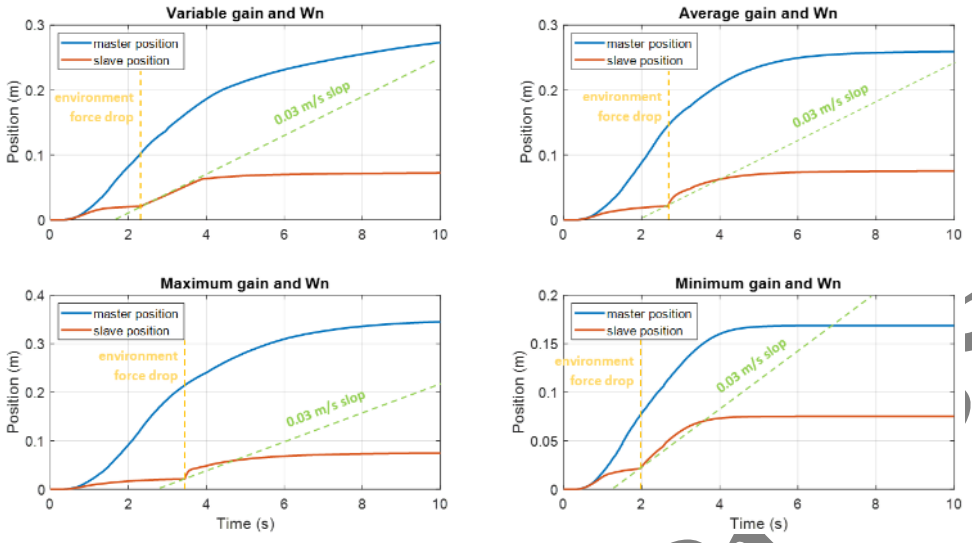

Fig 13: master and slave robots' positions during the whole operation using the proposed method

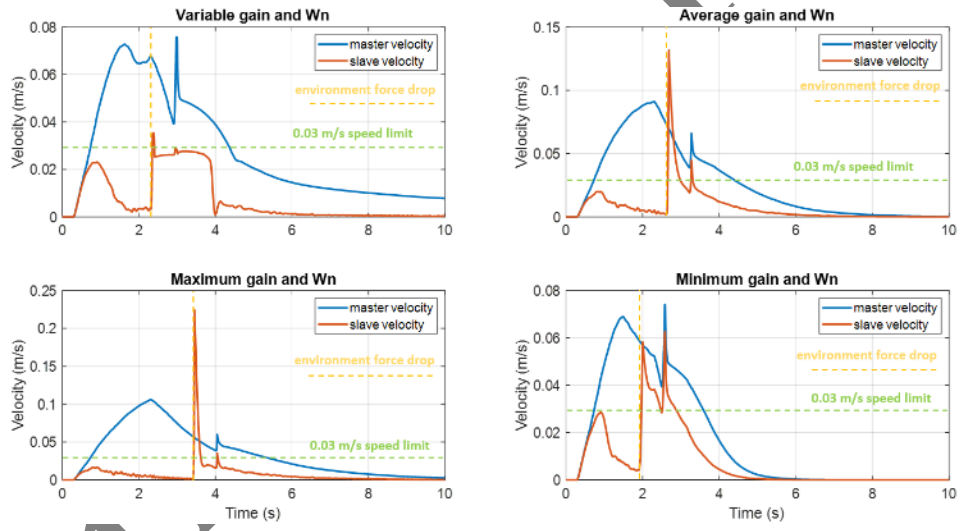

Fig 14: master and slave robots' velocities during the whole operation using the proposed method

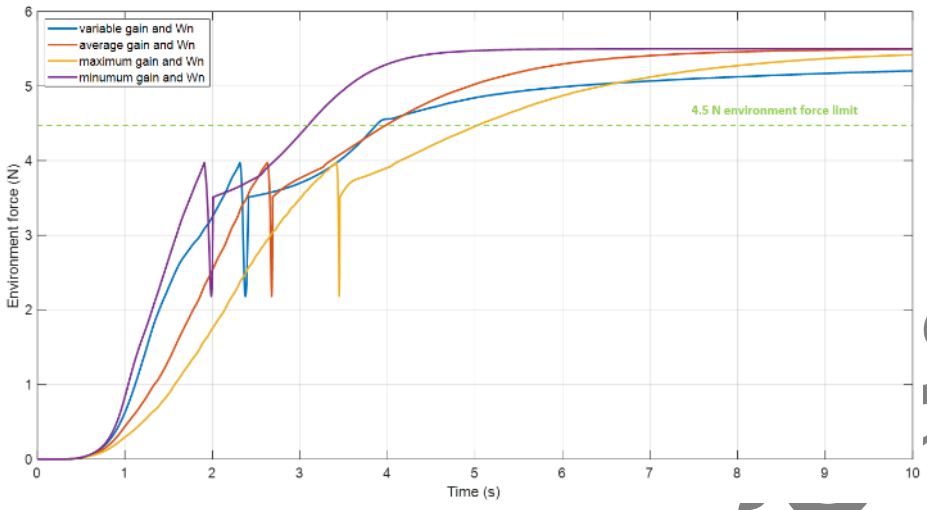

Fig 15: environment force during the whole operation using the proposed method

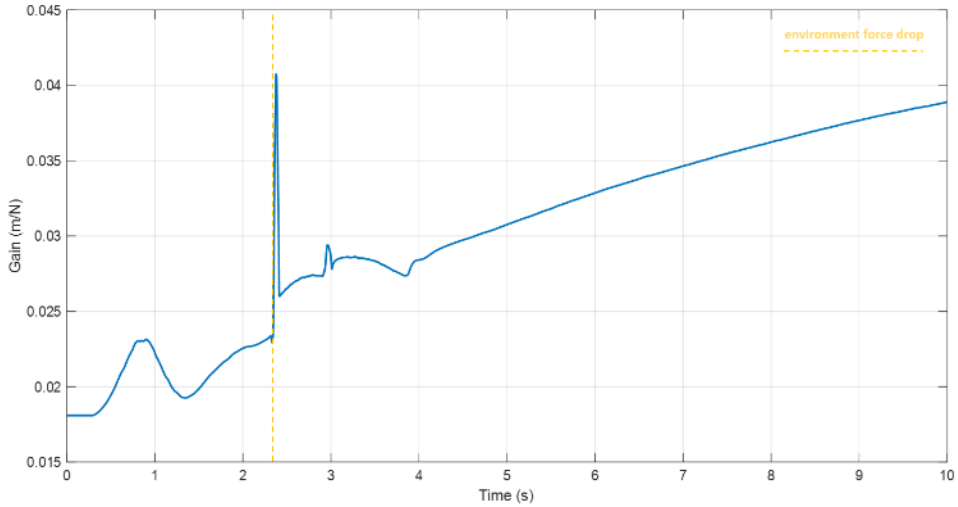

Fig 16: *gain* variation during the whole operation using the proposed method

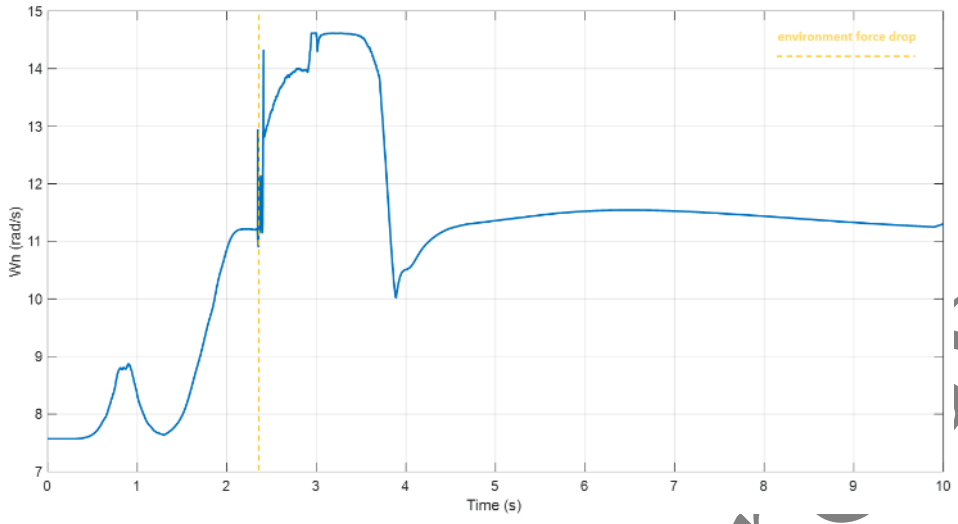

Fig 17: ω_n variation during the whole operation using the proposed method

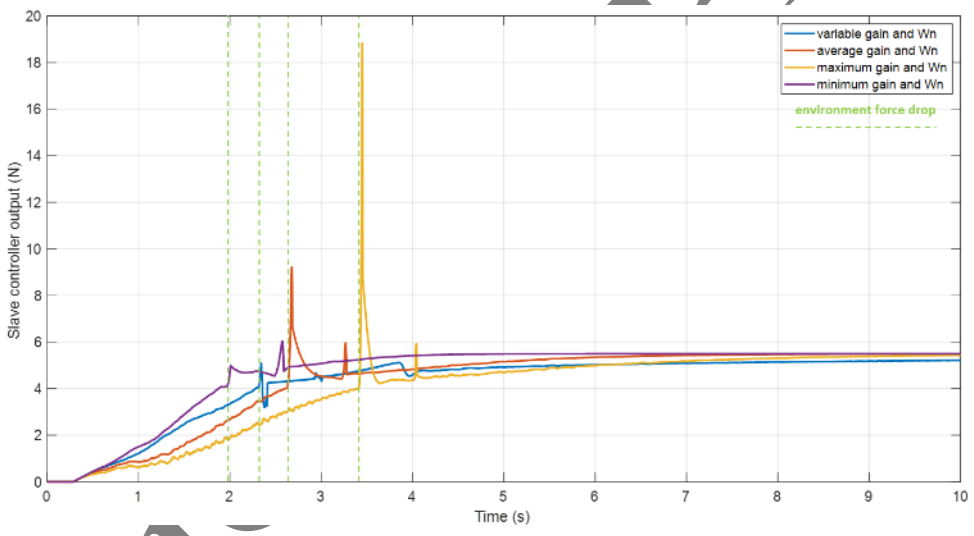

Fig 18: slave controller output during the whole operation using the proposed method

In **Error! Reference source not found.**, master and slave positions in four different cases are illustrated. The first case is the result of the proposed variable impedance control, in the second case ω_n and $gain$ are constant and are equal to the average amount of the chosen interval i.e. $11\ rad/s$ and $0.0335\ m/N$. In the third case ω_n and $gain$ are constant and are equal to the maximum amount of the chosen interval i.e. $15\ rad/s$ and $0.05\ m/N$. In the fourth case ω_n and $gain$ are constant and are equal to the minimum amount of the chosen interval i.e. $7\ rad/s$ and $0.017\ m/N$. Master position is different in all four cases because in the closed loop system, ω_n and $gain$ value and environment force affect the master position in addition to operator force.

In **Error! Reference source not found.**, master and slave velocities are illustrated. As can be seen the only case which satisfies the velocity limit is the proposed variable impedance control i.e. the first case. In all cases, when the environment force drops, the slave robot velocity increases suddenly, but the increase does not exceed the $0.03\ m/s$ limit with the proposed control method.

In **Error! Reference source not found.**, environment force in four cases is illustrated. Because the operator force equals 5.5 N after t = 2 s, the slave robot will not stop going forward until the environment force reaches 5.5 N. The environment force between constant cases reaches 5.5 N sooner in the minimum case and reaches 5.5 N later in the maximum case. In the variable case, after the environment force reaches the 4.5 N limit, the environment force increases as slowly as possible, and the slave position error keeps getting larger as the environment force increases.

In **Error! Reference source not found.** the gain value calculated by the fuzzy logic is illustrated. At the time when the environment force drops, a larger gain is chosen to keep the slave robot velocity under the 0.03 m/s limit.

In **Error! Reference source not found.** the ω_n value calculated by the fuzzy logic is illustrated. At the time when environment force drops, larger ω_n is chosen to reach faster to the error position.

In **Error! Reference source not found.** the slave controller output is illustrated. In all four cases a sudden increase can be seen when the environment force drop happens. But the maximum and average case reaches a high amount that can saturate the actuator. The variable case works with the lowest controller output.

6. Conclusion

In this paper, a novel variable impedance control method for a linear 1-DOF teleoperation system with time-varying delays is proposed with the goal of preventing the environment damage. First the coefficients of the desired impedance equation for the slave robot are converted from $\bar{m}_s$, $\bar{b}_s$ and $\bar{k}_s$ to ω_n, $gain$ and ζ. Then by considering ζ=1, ω_n and $gain$ are the parameters that are going to change. By considering the problem condition and absolute stability criteria, a desired interval for ω_n and $gain$ are defined, and then the frequency of the system is defined. By using fuzzy logic and getting environment force and slave robot's velocity as inputs, ω_n and $gain$ are changed in the defined interval as outputs. The fuzzy logic rules are designed to keep the environment force and slave robot's velocity at the limit which the environment can tolerate.

At the end, the proposed method is simulated and is compared to the same condition with constant impedance control. The results show that the proposed method keeps the environment force and slave robot's velocity at the defined limits and prevents any potential damage, whereas, in the constant impedance control case, the limits are exceeded and can cause damage, especially when there is a sudden fall in the environment force magnitude.

To clarify future contributions, applying the proposed control method to n-DOF and/or nonlinear manipulators is an important part that we consider. Advancing the proposed control strategy to the case where uncertainty in robot kinematics and dynamics exists is another future work that should be emphasized. Moreover, applying the proposed method in this paper to a real-life teleoperation setup is another future direction we consider working on.

References

[1] W. Liu, J. Zhang, L. Gao, Fuzzy impedance and sliding mode bilateral control in underwater ratio teleoperation based on observer, in *OCEANS 2016 - Shanghai*, 2016, pp. 1-7.

[2] X. Zhou, Z. Yang, Y. Ren, W. Bai, B. Lo, E. M. Yeatman, Modified Bilateral Active Estimation Model: A Learning-Based Solution to the Time Delay Problem in Robotic Tele-Control, *IEEE Robotics and Automation Letters*, Vol. 8, No. 5, pp. 2653-2660, 2023.

[3] M. Kadkhodazade, M. Pourmokhtari, B. Yazdankhoo, B. Beigzadeh, The Influence of Sex Factor on the Modeling of the Human Hand/Arm Interacting with a Teleoperation System, *Journal of Mechanics in Medicine and Biology*, 2023.

[4] A. Alfi, A. Bakhshi, M. Yousefi, H. A. Talebi, Design and Implementation of Robust-Fixed Structure Controller for Telerobotic Systems, *Journal of Intelligent & Robotic Systems*, Vol. 83, No. 2, pp. 253-269, 2016/08/01, 2016.

[5] P. Ji, F. Ma, F. Min, Terminal Traction Control of Teleoperation Manipulator With Random Jitter Disturbance Based on Active Disturbance Rejection Sliding Mode Control, *IEEE Access*, Vol. 8, pp. 220246-220262, 2020.

[6] B. Yazdankhoo, F. Najafi, M. R. Hairi Yazdi, B. Beigzadeh, Position synchronization for an uncertain teleoperation system with time delays using L1 theory, *Scientia Iranica*, Vol. 30, No. 1, pp. 16-29, 2023.

[7] B. Yazdankhoo, M. Nikpour, B. Beigzadeh, A. Meghdari, Improvement of Operator Position Prediction in Teleoperation Systems with Time Delay: Simulation and Experimental Studies on Phantom Omni Devices, *JJMIE*, Vol. 13, No. 3, 2019.

[8] M. Nikpour, B. Yazdankhoo, B. Beigzadeh, A. Meghdari, Adaptive online prediction of operator position in teleoperation with unknown time-varying delay: simulation and experiments, *Neural Computing and Applications*, 2020.

[9] B. Yazdankhoo, B. Beigzadeh, Increasing stability in model-mediated teleoperation approach by reducing model jump effect, *Scientia Iranica*, Vol. 26, No. Special Issue on: Socio-Cognitive Engineering, pp. 3-14, 2019.

[10] Y. Zhu, K. Fusano, T. Aoyama, Y. Hasegawa, Intention-reflected predictive display for operability improvement of time-delayed teleoperation system, *ROBOMECH Journal*, Vol. 10, No. 1, pp. 17, 2023/07/15, 2023.

[11] P. M. Kebria, A. Khosravi, S. Nahavandi, Neural Network Control of Teleoperation Systems with Delay and Uncertainties based on Multilayer Perceptron Estimations, in *2020 International Joint Conference on Neural Networks (IJCNN)*, 2020, pp. 1-7.

[12] A. Mehrjouyan, M. B. Menhaj, M. A. Khosravi, Robust observer-based adaptive synchronization control of uncertain nonlinear bilateral teleoperation systems under time-varying delay, *Measurement*, Vol. 182, pp. 109542, 2021/09/01/, 2021.

[13] E. Franco, Combined Adaptive and Predictive Control for a Teleoperation System with Force Disturbance and Input Delay, *Frontiers in Robotics and AI*, Vol. 3, 2016-August-10, 2016. English

[14] J. Wang, J. Tian, X. Zhang, B. Yang, S. Liu, L. Yin, W. Zheng, Control of Time Delay Force Feedback Teleoperation System With Finite Time Convergence, *Frontiers in Neurorobotics*, Vol. 16, 2022-May-06, 2022. English

[15] Y. Michel, R. Rahal, C. Pacchierotti, P. R. Giordano, D. Lee, Bilateral Teleoperation With Adaptive Impedance Control for Contact Tasks, *IEEE Robotics and Automation Letters*, Vol. 6, No. 3, pp. 5429-5436, 2021.

[16] B. Yazdankhoo, M. R. Ha'iri Yazdi, F. Najafi, B. Beigzadeh, L1 impedance control for bilateral teleoperation containing model uncertainty, *Transactions of the Institute of Measurement and Control*, Vol. 44, No. 16, pp. 3154-3164, 2022.

[17] J. Zhang, H. Li, Y. Song, B. Su, S. Li, The Model Reference Adaptive Impedance Control Scheme in Underwater Manipulator Bilateral Teleoperation System Under Model Uncertainty and External Disturbance, in *Proceedings of 2022 Chinese Intelligent Systems Conference*, Singapore, 2022, pp. 825-833.

[18] S. H. Tabatabaei, A. H. Zaeri, M. Vahedi, Design an impedance control strategy for a teleoperation system to perform drilling process during spinal surgery, *Transactions of the Institute of Measurement and Control*, Vol. 41, No. 10, pp. 2947-2956, 2019.

[19] T. Wang, Y. Li, J. Zhang, Y. Zhang, A novel bilateral impedance controls for underwater tele-operation systems, *Applied Soft Computing*, Vol. 91, pp. 106194, 2020/06/01/, 2020.

[20] F. J. Abu-Dakka, M. Saveriano, Variable Impedance Control and Learning—A Review, *Frontiers in Robotics and AI*, Vol. 7, 2020-December-21, 2020. English

[21] J. Duan, Y. Gan, M. Chen, X. Dai, Adaptive variable impedance control for dynamic contact force tracking in uncertain environment, *Robotics and Autonomous Systems*, Vol. 102, pp. 54-65, 2018/04/01/, 2018.

[22] Z. Ma, D. Shi, Z. Liu, J. Yu, P. Huang, A Bilateral Teleoperation System With Learning-Based Cognitive Guiding Force, *IEEE Transactions on Cognitive and Developmental Systems*, Vol. 15, No. 4, pp. 2214-2227, 2023.

[23] M. Aghaseyedabdollah, M. Abedi, M. Pourgholi, Supervisory adaptive fuzzy sliding mode control with optimal Jaya based fuzzy PID sliding surface for a planer cable robot, *Soft Computing*, Vol. 26, No. 17, pp. 8441-8458, 2022/09/01, 2022.

[24] Y. Bouteraa, K. A. Alattas, T. Peng, A. Fekih, R. Rahmani, S. Mobayen, Design of robust adaptive fuzzy control for uncertain bilateral teleoperation systems based on backstepping approach, *IET Control Theory & Applications*, Vol. 17, No. 7, pp. 800-813, 2023.

[25] T. Sutikno, A. C. Subrata, A. Elkhateb, Evaluation of Fuzzy Membership Function Effects for Maximum Power Point Tracking Technique of Photovoltaic System, *IEEE Access*, Vol. 9, pp. 109157-109165, 2021.

[26] F. Khadivar, S. Sadeghnejad, H. Moradi, G. Vossoughi, F. Farahmand, Dynamic Characterization of a Parallel Haptic Device for Application as an Actuator in a Surgery Simulator, in *2017 5th RSI International Conference on Robotics and Mechatronics (ICRoM)*, 2017, pp. 186-191.

[27] Q. Q. Cheng, P. X. Liu, P. H. Lai, Y. N. Zou, An Interactive Meshless Cutting Model for Nonlinear Viscoelastic Soft Tissue in Surgical Simulators, *IEEE Access*, Vol. 5, pp. 16359-16371, 2017.